INTERNATIONAL ATOMIC ENERGY AGENCY
UNITED NATIONS EDUCATIONAL, SCIENTIFIC AND CULTURAL ORGANIZATION

INTERNATIONAL CENTRE FOR THEORETICAL PHYSICS
34100 TRIESTE (ITALY) - P.O.B. 586 - MIRAMARE - STRADA COSTIERA 11 - TELEPHONE: 2240-1
CABLE: CENTRATOM - TELEX 460392-1

H4.SMR/204 - 30

WINTER COLLEGE ON

ATOMIC AND MOLECULAR PHYSICS

(9 March - 3 April 1987)

PLASMA DIAGNOSTICS

C.S. Wong

Institüt für Plasmaforschung
Universität Stuttgart
Pfaffenwaldring 31
7000 Stuttgart 80
Federal Rep. of Germany

Permanent address

Plasma Research Laboratory
Physics Dept.
University of Malaya
Kuala Lumpur
Malaysia

Winter College on Atomic and Molecular Physics
ICTP, Trieste, Italy. March 9 – April 3, 1987.

PLASMA DIAGNOSTICS

C.S.Wong

1. Rogowski Coil

2. Magnetic Probe

3. High Voltage Probe
   resistive divider
   capacitive divider

4. Electric Probe
   single and double probes
   computer controlled system
   pulsed system
   triple probe

Emphases given to : basic principles
application examples

PRINCIPLE OF ROGOWSKI COIL :

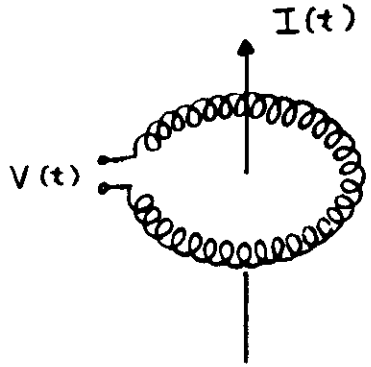

$B = \frac{\mu_0 I}{2\pi r}$

Voltage induced :

$$V(t) = \left(\frac{\mu_0 NA}{2\pi r}\right) \frac{dI}{dt}$$

where N is no. of turns;
A is the minor cross-sectional area; and
r is the major radius of the torus.

2 MODES OF OPERATION :

(1) With RC-integrator

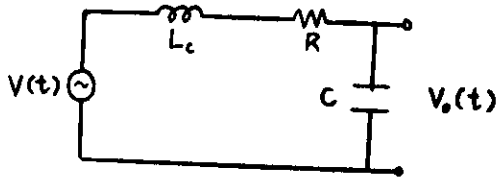

$$V_o(t) = \left(-\frac{\mu_o NA}{2\pi rRC}\right) I(t)$$

with $RC >> \omega^{-1}$; and

$R >> \omega L_c$

(2) Self-integrating(current transformer)

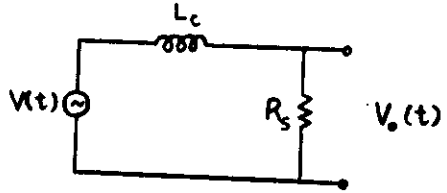

$$V_o(t) = \left(-\frac{R_s}{N}\right) I(t)$$

with $R_s << \omega L_c$

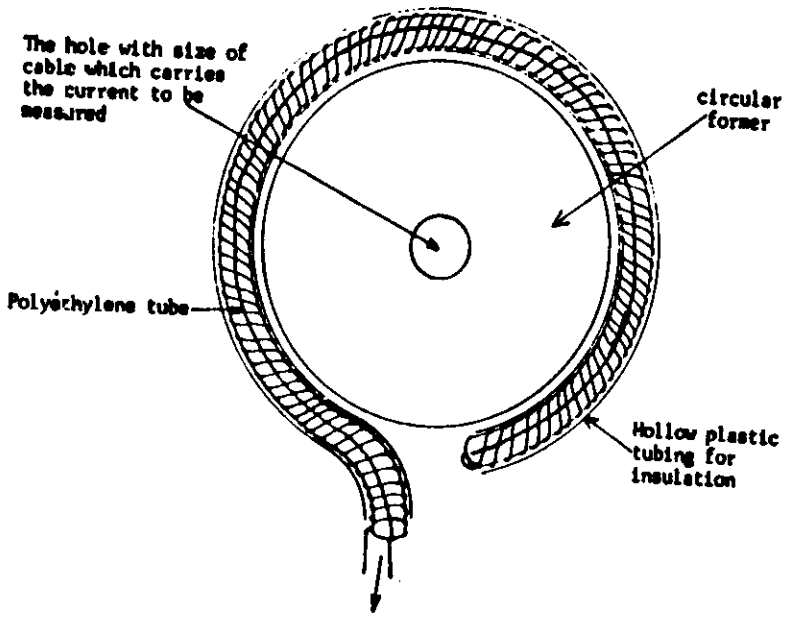

Fig. 3.1 The construction of a Rogowski coil. (C.Y. Ong, M.Sc. Thesis)

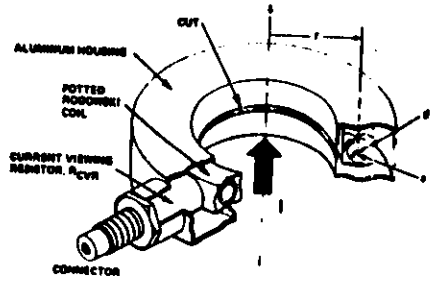

D.G. Pellinen et. al.
Rev. Sci. Instrum 51, 1535 (1980)

RESPONSE OF ROGOWSKI COIL

For self-integrating coil :

$2\tau < t_r < L_c/R_s$

τ is transit time of signal along coil.

For a coil with electrostatic shielding,

$\tau = \sqrt{(LC)} \cdot 2\pi r$

where L, C are inductance and capacitance per unit length of the coil.

Factors affecting response :

1. $R_s > \sqrt{(L/C)}$.
   - $V_o(t)$ becomes oscillatory.
2. Imperfect R_s
   - $V_o(t)$ becomes oscillatory.
3. Skin effect (high frequency I).
   L increases => τ increases.

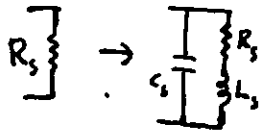

For RC-integrator mode :

$L_c/R < t_r < RC$

If long connecting cable with impedence Z is used, then R = Z (usually 50Ω);

and $t_r > L_c/50$.

$L_c \sim \mu H$ => $t_r \sim \mu s$

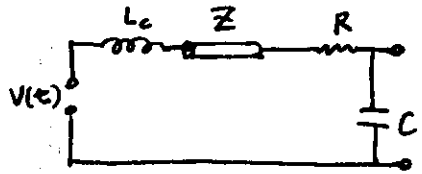

DDAII CDC 01/25/87 13.43.55.

CALIBRATION OF ROGOWSKI COIL :

- best done in situ using an ideal LCR discharge

For a LCR discharge,

$I(t) = I_o \exp(-\alpha t)\sin \omega t$

where $I_o = V_o \sqrt{(C/L)}$

$\alpha = R/(2L)$

$\omega = 1/\sqrt{LC}$

From current waveform obtained,

$$\alpha = -\frac{\ln (V_2/V_1)}{T}$$

V_1 - $I_1 = I_o \exp(-\alpha T/4)$

Coil constant :

$$K_I = \frac{2\pi C V_o}{T V_1} \left(\frac{V_2}{V_1}\right)^{1/4}$$

C, V_b are known; and V_1 , V_2 , T are measured from waveform

DDAII CDC 01/21/87 16.07.55.

THE MAGNETIC PROBE

1. Principle – same as Rogowski coil
   Voltage induced :

$$V(t) = NA\left(\frac{dB}{dt}\right)$$

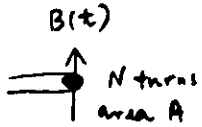

2. Small in size
   - measure localised field
     hence field distribution

3. L_c small
   $R_s << \omega L_c$ only true at large ω
   => Self integrating mode not possible
   With RC integrator,

$$V_o(t) = \left(\frac{NA}{RC}\right) B(t)$$

4. Response : $L_c/Z < t_r < RC$

5. Electrostatic shielding
   - against capacitive pick-up
     of high frequency plasma potential

DDAII CDC

HIGH VOLTAGE PROBE

1. Resistive divider

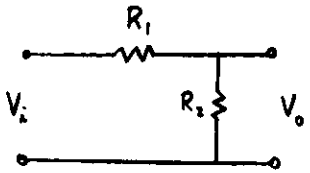

$$\frac{V_o}{V_i} = \frac{R_2}{R_1 + R_2}$$

2. Capacitive divider

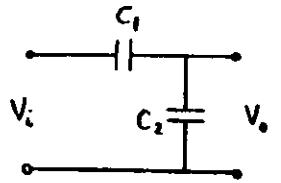

$$\frac{V_o}{V_i} = \frac{C_1}{C_1 + C_2}$$

3. Hybrid : capacitive-resistive

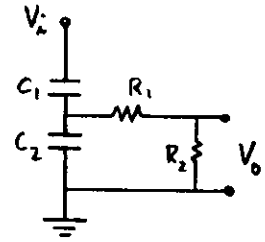

$$\frac{V_o}{V_i} = \left(\frac{C_1}{C_1 + C_2}\right)\left(\frac{R_2}{R_1 + R_2}\right)$$

4. Hybrid : capacitive//resistive

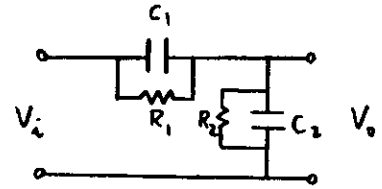

$$\frac{V_o}{V_i} = \frac{C_1}{C_2} = \frac{R_2}{R_1}$$

DDAII CDC
01/25/87 15.50.37.

THE RESISTIVE PROBE

An example :

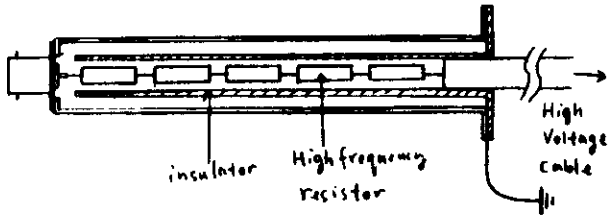

Probe response affected by :

(i) Stray inductance.

$t_r > L_s/R_2$

$R_2 = 50\ \Omega$

For $L_s \sim \mu H \Rightarrow t_r > 100$ ns

For $L_s \sim 10$ nH $\Rightarrow t_r >$ ns

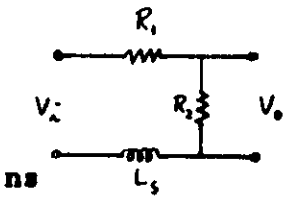

(ii) Stray capacitance.

$t_r > R_1 C_s$

For $C_s \sim$ pF $\Rightarrow t_r >$ ns

For $C_s \sim$ nF $\Rightarrow t_r > \mu$s

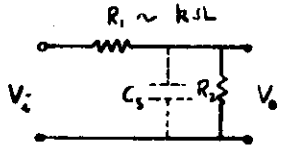

(iii) Transit time.

$t_r > \sqrt{(LC)}\ .\ l$

Shielding may increase L and C

THE CAPACITIVE PROBE

Factors affecting response :

1. Stray inductance.

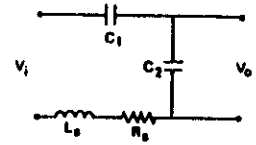

Natural frequency : $\omega_o = 1/\sqrt{(L_s C)}$

$C = C_1 C_2/(C_1 + C_2)$

Upper frequency limit : $\omega < \omega_o$

2. Terminating impedance.

Lower frequency limit : $\omega > 1/ZC_2$

Connect direct to scope output,

$Z = 1\ M\Omega$

Take $C_2 = 100$ pF

$\Rightarrow \omega > 10$ kHz

When long cable connection required, need to couple to a resistive stage --> capacitive-resistive probe

3. Transit time.

$t_r > \sqrt{(LC)}\ .\ l$

EFFECT OF STRAY INDUCTANCE

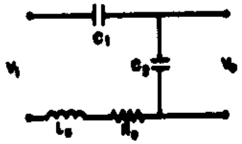

FIG. 1. The [illegible]

Circuit equation:

$$L_s\frac{d^2Q}{dt^2} + R_s\frac{dQ}{dt} + \frac{Q}{C} = V_i$$

where $C = C_1C_2/(C_1 + C_2)$

Take $V_i = V_m \sin(\omega t)$

Let $\tau = t/\surd(L_sC)$; $q = Q/Q_o$; $\delta_s = R_s/\surd(L_s/C)$;

$\gamma = \omega/\omega_o$; $\omega_o = 1/\surd(L_sC)$; $Q_o = CV_m$

Then $$\frac{d^2q}{d\tau^2} + \delta_s\left(\frac{dq}{d\tau}\right) + q = \sin(\gamma\tau)$$

Solution: $$q(\tau) = \left(\frac{1}{1-\gamma^2}\right)[\sin(\gamma\tau) - \sin\tau] \quad (\delta_s \simeq 0)$$

Output voltage: $v_o(\tau) = \beta q(\tau)$

where $\beta = C_1/(C_1+C_2)$

Rev. Sci. Instrum. 56, 761 (1985) Fig. 1(a)

CAPACITIVE DIVIDER FROM COAXIAL CABLE

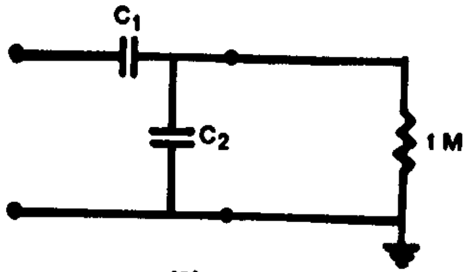

(a)

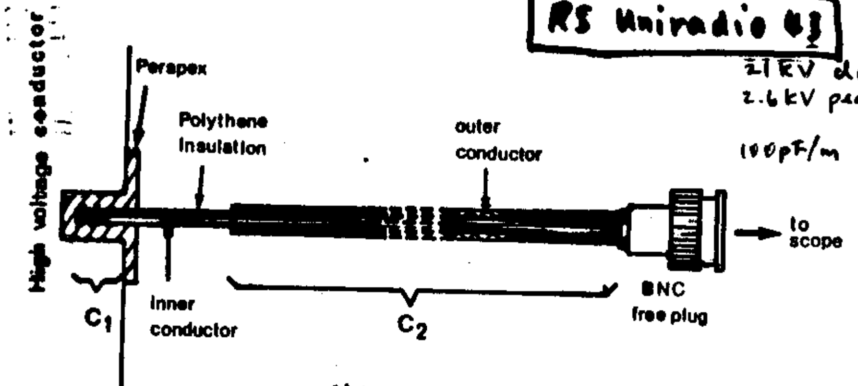

(b)

RS Uniradio 43

21 kV dc
2.6 kV peak rf (cw)
100 pF/m

RSI/[illegible]/MAY 85/Fig. 1/f: 55 %

CAPACITIVE-RESISTIVE PROBE

2 possible modes :

(i) $(R_1 + R_2)C_2 > \tau$

where τ is characteristic time of interest

==> voltage divider mode

$V_o \propto V_i$

(ii) $(R_1 + R_2)C_2 < \tau$

==> differentiator mode

$V_o \simeq R_2 C_1 (dV_i/dt)$

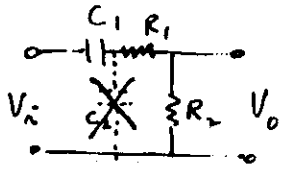

For $(R_1 + R_2)C_2 \simeq \tau$

==> mixture of 2 modes

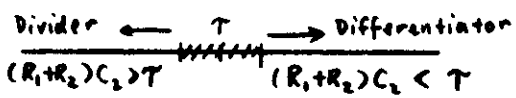

Requirement of long connecting cable,

==> $R_2 = 50\ \Omega$

Then with $R_1 = 5000\ \Omega$

and $C_2 = 100$ pF,

the probe acts as voltage divider only for voltage pulses with $\tau < 500$ ns

CAPACITIVE//RESISTIVE PROBE

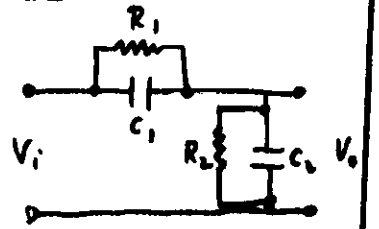

1. Required to fix $\frac{R_2}{R_1} = \frac{C_1}{C_2}$

   Take $R_2 = 50\ \Omega$ (cable impedance),

   $C_1 = 10$ pF,

   $C_2 = 100$ pF,

   ==> $R_1 = 500\ \Omega$

2. For $\omega > 1/R_1C_1$,

   ==> capacitive

3. For $\omega < 1/R_1C_1$,

   ==> resistive

4. For $\omega \simeq 1/R_1C_1$,

   Response of the probe may be nonlinear(?)

5. Upper frequency limit

   Set by either transit time, or stray inductance

   (Refer to capacitive probe)

PLASMA AS ACTIVE CIRCUIT ELEMENT

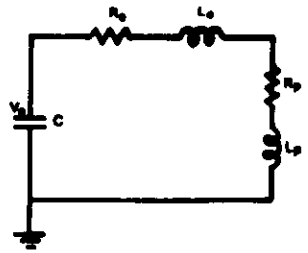

L_e : circuit inductance
R_e : circuit resistance
$L_p(t)$: plasma inductance
$R_p(t)$: plasma resistance

Circuit equation :

$$V_o - \frac{\int I\,dt}{C} = \frac{d}{dt}\left[(L_e + L_p)I\right] + I(R_e + R_p)$$

R_e is usually negligible

Voltage across plasma :

$$V_p(t) = \frac{d}{dt}(L_p I) + IR_p$$

DEDUCTION FROM I(t)

1. Ideal LCR discharge (calibration)

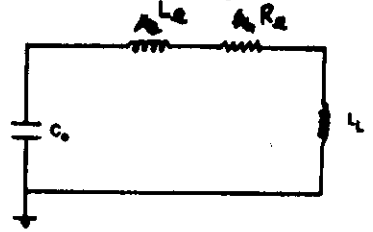

Measure T and α from I(t)
$T = 2\pi\sqrt{(LC)}$, $L = L_e + L_L$
C and L_L are known
==> L_e, the circuit inductance

$\alpha = R_e/(2L)$, the damping factor
==> R_e, the circuit resistance

2. Plasma discharge
Voltage across plasma :

$$V_p(t) = V_o - \frac{\int I\,dt}{C} - L_e\frac{dI}{dt}$$

-- dependent on $\int I dt$ and dI/dt

From I(t) measured, obtain $\int I dt$ and dI/dt
==> $V_p(t)$, the plasma voltage waveform

ENERGY CONSIDERATION

Rate of electrical energy input :

$$W_e = I(t)V_p(t)$$
$$= I^2\frac{dL_p}{dt} + L_pI(\frac{dI}{dt}) + I^2R_p$$

Magnetic energy : $E_m = L_pI^2/2$

Rate of change : $W_m = \frac{I^2}{2}(\frac{dL_p}{dt}) + L_pI(\frac{dI}{dt})$

Hence rate of energy input to the plasma :

$$W_p = \frac{I^2}{2}(\frac{dL_p}{dt}) + I^2R_p$$

(dynamic) (Joule)

Dynamic – compression or expansion(configuration)
Joule heating – due to resistivity

At any instant t, from I(t) and $V_p(t)$,
E_e, E_m and E_p can be calculated

DEDUCTION FROM I(t) AND $V_p(t)$

With I(t) measured; and $V_p(t)$ measured
or deduced from I(t)

1. Assume plasma to be INDUCTIVE
   Plasma inductance :
   $$L_p(t) = \frac{\int V_p dt}{I}$$
   L_p is related to geometry of plasma.
   e.g. the linear Z-pinch
   $$L_p(t) = \frac{\mu_0 l}{2\pi} ln(\frac{r_e}{r})$$
   for coaxial geometry
   $$==> r(t) = r_e \exp(-\frac{2\pi L_p}{\mu_0 l})$$
   -- the plasma trajectory
2. If plasma is RESISTIVE
   i.e. $R_p >> \omega L_p$, or L_p is fixed
   Bulk plasma resistance :
   $$R_p(t) = [V_p(t) - L_p(dI/dt)]/I(t)$$
   Plasma conductivity $\sigma = l/(R_pA)$
   $\sigma \propto T_e^{3/2}$
   ==> T_e, the electron temperature
   e.g. Coaxial flashlamp

CONCEPT OF PLASMA POTENTIAL

In an ideal plasma,
charge neutrality ==> zero electrostatic field

But, the system of particles possesses
potential energy
Plasma at potential ϕ_s with respect to ground

2 consequences :

(i) If an external charge is placed into the plasma, the plasma particles re-distribute to shield off the effect of the alien particle to within a distance λ_D from the particle.
(Debye shielding)

$$\lambda_D = 6.9\sqrt{\left[\frac{T}{(1+Z)n_e}\right]}$$

(ii) Imagine the alien particle suddenly disappears, then the system of particles try to restore equilibrium.
==> oscillation about equilibrium with frequency

$$\omega_p = \sqrt{\left(\frac{n_e e^2}{\varepsilon_0 m_e}\right)}$$

ASSUMPTIONS OF PROBE THEORY

1. Plasma is infinite, homogeneous and neutral
2. Particles have Maxwellian velocity distn.
3. No collision between particles within the viscinity of the probe
4. Particles hitting the probe are absorbed (no deflection, no emission of particle)
5. The bulk of the plasma is not disturbed by the presence of the probe
6. No strong magnetic field in the plasma

FLOATING CONDUCTOR IN PLASMA

At equilibrium,

-- the conductor becomes negatively charged due to electron attachment.

-- at floating potential ϕ_f (negative)

-- shielded by positive plasma sheath from the bulk of the plasma.
(no. ions > no. electrons in the sheath)

-- thickness of the sheath = λ_D

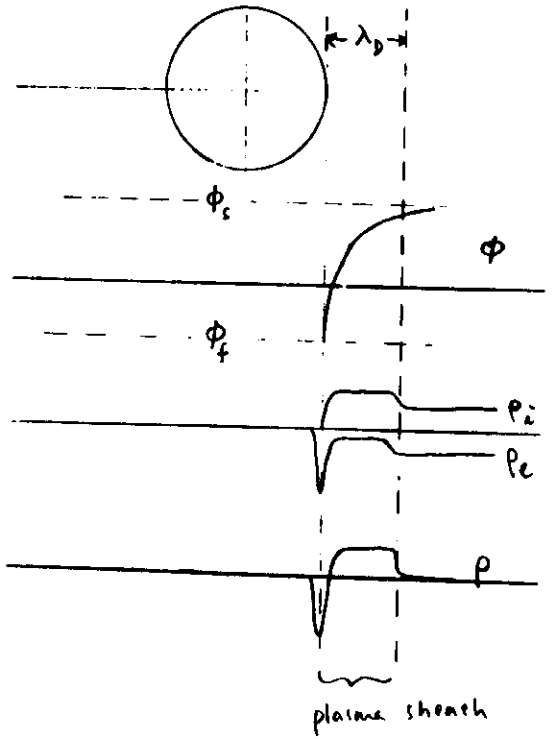

DDAII CDC 02/05/87 16.45.40.

MEASUREMENT OF FLOATING POTENTIAL

For d.c. plasma (e.g. glow discharge)

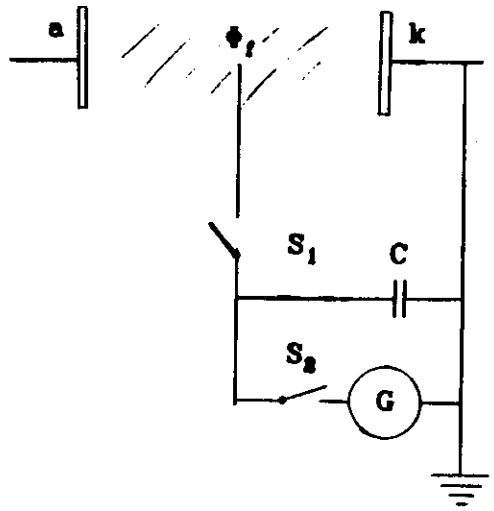

When S_1 is closed,
capacitor C charged to potential ϕ_f

Then open S_1, and close S_2;
C discharged through galvanometer G
Deflection = $k(C\phi_f)$

k can be obtained by calibration using a known voltage source

DDAII CDC 02/08/87 09.34.52.

BIASED CONDUCTOR (PROBE) IN PLASMA

1. $\phi_p < \phi_f$ (ion saturation region)
   $I_p = i_{ri}$, constant

2. $\phi_p \rightarrow \phi_f$
   no. of e reaching probe increases
   I_p decreases ($I_p = i_{ri} - i_e$)

3. $\phi_p = \phi_f$
   $I_e = i_{ri} \Rightarrow I_p = 0$

4. $\phi_f < \phi_p < \phi_s$ (e retardation region)
   more e are reaching the probe
   but they are retarded by the field

5. $\phi_p > \phi_s$ (e acceleration region)
   $I_p = i_{re}$

6. $\phi_p >> \phi_s$ (secondary emission region)
   e accelerated to high energy
   secondary particle emission from probe surface
   --> probe starts to glow
   I_p becomes very large

THE SINGLE PROBE

(The e retardation region)

For this region, electron current given by:

$$i_e = i_{re} \exp\left[- \frac{e(\phi_s - \phi_p)}{kT_e} \right]$$

Probe current $I_p = i_e - i_{ri}$

From probe characteristic : (ϕ_p, I_p),
--> (ϕ_p, i_e)

Plot $\ln i_e$ vs ϕ_p

Gradient = e/kT_e

==> T_e, the electron temperature

At $\phi_p = \phi_s$ obtain i_{er}

$$i_{er} = An_e e \sqrt{\left(\frac{kT_e}{2\pi m_e}\right)}$$

==> n_e, the electron density

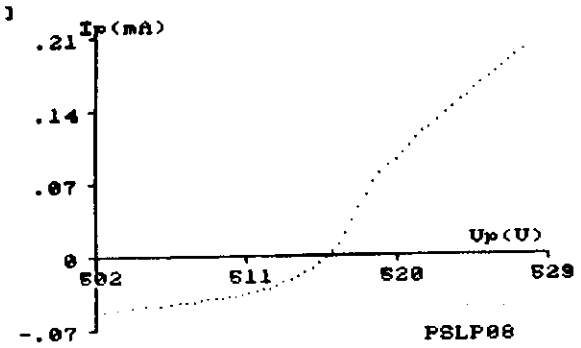

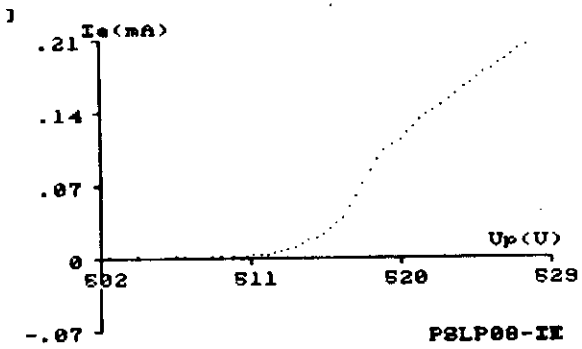

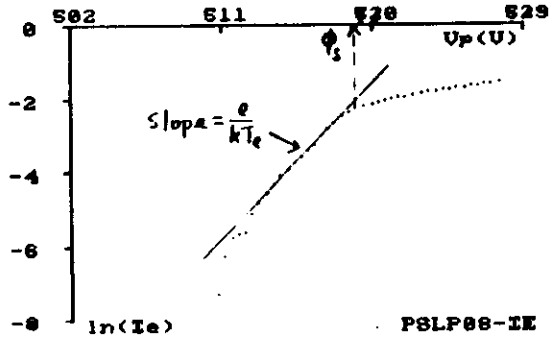

POSSIBLE COMPLICATIONS

1. i_{ri} is not constant.

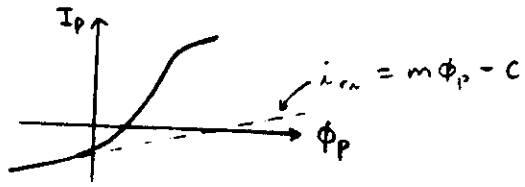

Then $i_{ri} = m\phi_p - c$
which is a linear function of ϕ_p

2. The point $\phi_p = \phi_s$ not clearly observed
-- determined from change of gradient

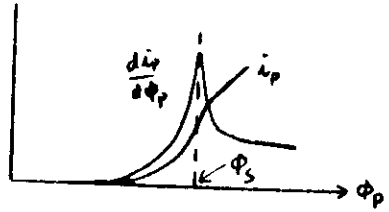

3. Absence of exponential e retardation region
==> plasma not Maxwellian

It is required to determine the EEDF before application of classical probe theory

EXPERIMENTAL DIFFICULTIES

1. Unsteady plasma condition.
   Impossible to complete a set of probe characteristic by the point-by-point method

   -- use pulsed probe

2. Probe contamination
   (gas molecules attachment; metallic coating)
   -- can be cleaned by sputtering

3. For plasma of temperature > 10 eV,
   ion bombardment of probe may occur
   --> secondary particles emission
   --> glow or arc between probe and plasma

4. Plasma perturbation
   condition of plasma obtained may differ from the actual condition

5. Electrons not completely absorbed
   -- e.g. reflection

6. Photoemission - due to uv

THE DOUBLE PROBE (1)

Ideally, assume
(i) 2 exactly identical probes
(ii) same space potential
Then,

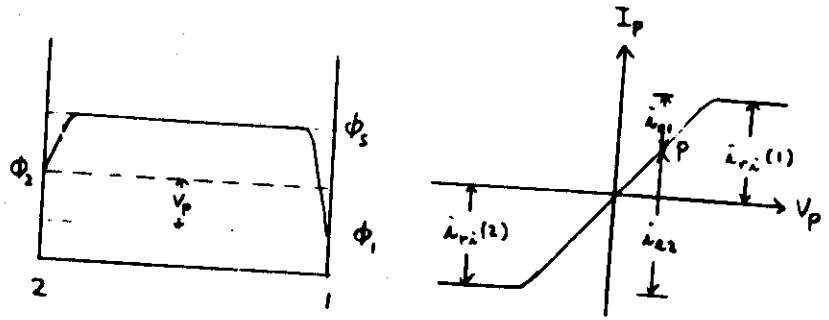

At P :

$$i_{e1} = i_{re} \exp\left[-\frac{e(\phi_s - \phi_1)}{kT_e}\right],\ i_{e1} = i_{r1} - I_p$$

$$i_{e2} = i_{re} \exp\left[-\frac{e(\phi_s - \phi_2)}{kT_e}\right],\ i_{e2} = i_{r1} + I_p$$

$$i_{e1} + i_{e2} = i_{r1}(1) + i_{r1}(2) = 2i_{r1}$$

$$1 + \frac{i_{e1}}{i_{e2}} = \frac{2i_{r1}}{i_{e2}}$$

$$\exp\left[-\frac{e(\phi_2 - \phi_1)}{kT_e}\right] = \frac{2i_{r1}}{I_p + i_{r1}} - 1 \qquad (V_p = \phi_2 - \phi_1)$$

THE DOUBLE PROBE (2)

Experimentally,

from the double probe characteristic,

-- **measure** i_{ri}

-- **obtain a set of points** $(V_p \ , \ I_p)$

-- **plot** $\ln\left[\frac{2i_{ri}}{I_p + i_{ri}} - 1\right]$ **vs** V_p

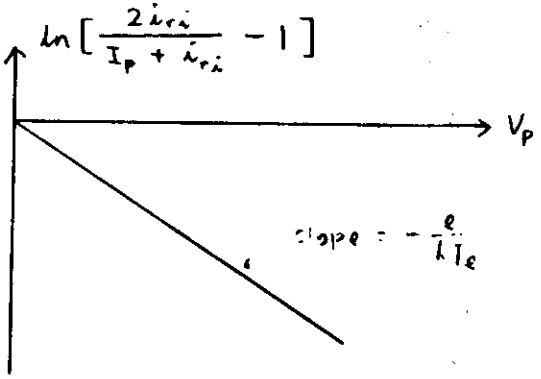

Slope = $- e/kT_e$

==> T_e**, the electron temperature**

COMPLICATIONS IN DOUBLE PROBE CHARACTERISTICS (1)

1. **Non-uniform space potential**

$$\Rightarrow \exp\left[-\frac{e(V_p - \phi_c)}{kT_e}\right] = \frac{2i_{ri}}{I_p + i_{ri}} - 1$$

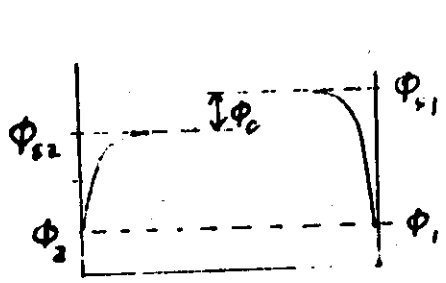

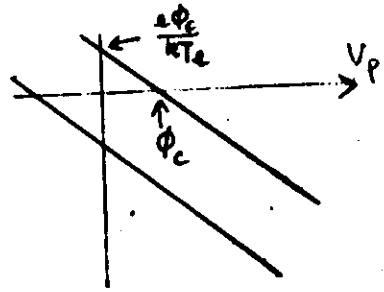

2. **Non-identical probe areas :** $A_1 \neq A_2$

$$\Rightarrow \left(\frac{A_2}{A_1}\right)\exp\left(-\frac{eV_p}{kT_e}\right) = \frac{2i_{ri}}{I_p + i_{ri}} - 1$$

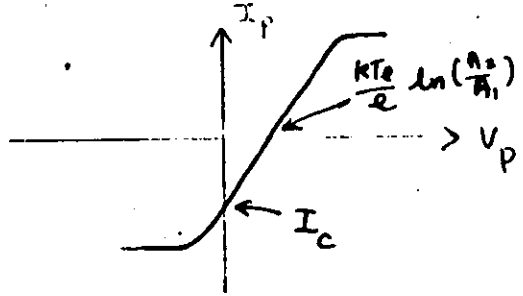

At $V_p = 0$, $I_p = \left(\frac{A_1 - A_2}{A_1 + A_2}\right) i_{ri}$

At $I_p = 0$, $V_p = \frac{kT_e}{e}\ln\left(\frac{A_2}{A_1}\right)$

- $i_{ri1} \neq i_{ri2}$

$$\Rightarrow \exp(-\frac{eV_p}{kT_e}) = \frac{i_{ri1} + i_{ri2}}{I_p + i_{ri2}} - 1$$

- In general, the experimental double probe characteristic can be given by :

$$(\frac{A_2}{A_1}) \exp[-\frac{e(V_p - \phi_c)}{kT_e}] = \frac{i_{ri1} + i_{ri2}}{I_p + i_{ri2}} - 1$$

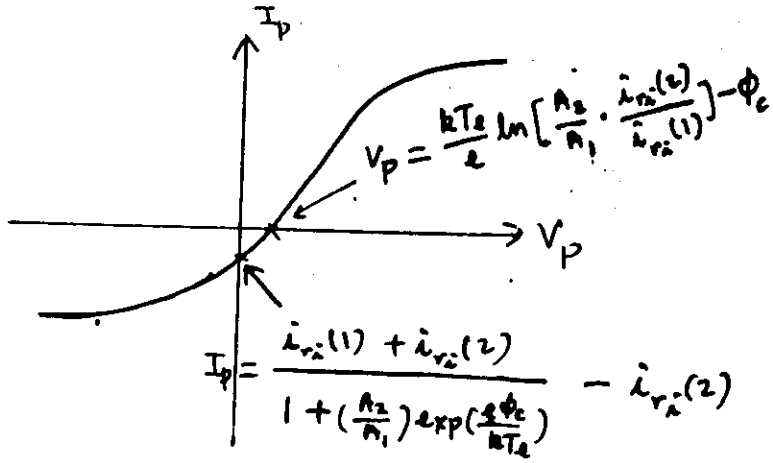

ortunately, T_e can still be determined from:

lot $\ln[\frac{i_{ri1} + i_{ri2}}{I_p + i_{ri2}} - 1]$ vs V_p

slope = $-\frac{e}{kT}$ $\Rightarrow$ T_e

ALTERNATIVE METHOD OF DOUBLE PROBE CHARACTERISTIC INTERPRETA

$$\frac{i_{e2}}{i_{e1}} = \frac{i_{ri2} + I_p}{i_{ri1} - I_p} = \frac{A_2}{A_1} \exp[-\frac{e(V_p - \phi_c)}{kT_e}]$$

Upon differentiation with respect to V_p,

$$\Rightarrow \frac{dI_p}{dV_p} = \frac{e}{kT_e} [\frac{(I_p + i_{ri2})(i_{ri1} - I_p)}{i_{ri1} + i_{ri2}}]$$

At $I_p = 0$,

$$(\frac{dI_p}{dV_p})_{I_p=0} = \frac{e}{kT_e} [\frac{i_{ri2} i_{ri1}}{i_{ri1} + i_{ri2}}]$$

From the probe characteristic,

measure i_{ri1}, i_{ri2} and $(\frac{dI_p}{dV_p})_{I_p=0}$ $\Rightarrow$ T_e

Assume $T_i \ll T_e$ and $n_e \simeq n_i$

then $i_{ri} \simeq 2An_e e / (kT_e/m_i)$; where $i_{ri} = \frac{1}{2}[i_{ri1} + i_{ri2}$

$\Rightarrow$ n_e

PROBE TECHNIQUES - IMPLEMENTATION

1. Manual, point-by-point
   - slow, tedeous, inaccurate

2. microcomputer-controlled data acquisition
   - require fast ADC and DAC
   - preferably 16-bits for better resolution

3. Pulsed system
   - for dc plasma, use ms sweep
     ==> probe characteristic captured in ms
   - can be extended to obtain (dI_p/dV_p) directly by using a simple RC differentiator
   - can also be coupled to a computer via a digitiser or an oscilloscope with digiter storage
   - sweeping rate limited to

$$\frac{dV}{dt} \leq \frac{i_{ri}}{C_s}$$

where C_s is the stray capacitance between the probe and the reference electrode (cathode or anode)

(a) Single

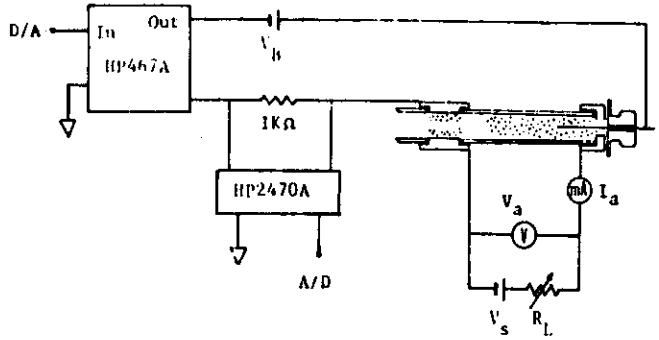

Fig. 2. Experimental set-up of the microcomputer-based Langmuir probe measurement of the glow discharge.

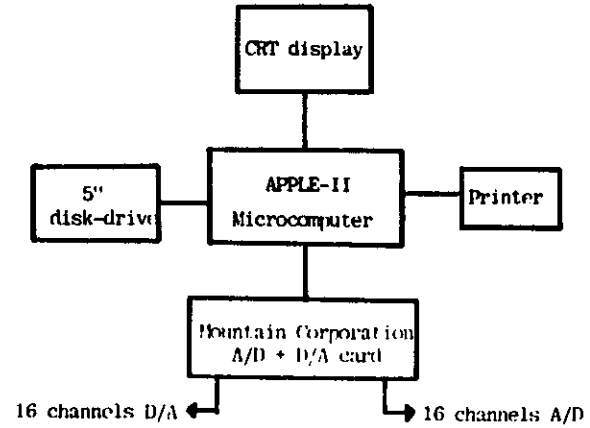

Fig. 3. Block diagram of the data acquisition system.

Microcomputer controlled double probe

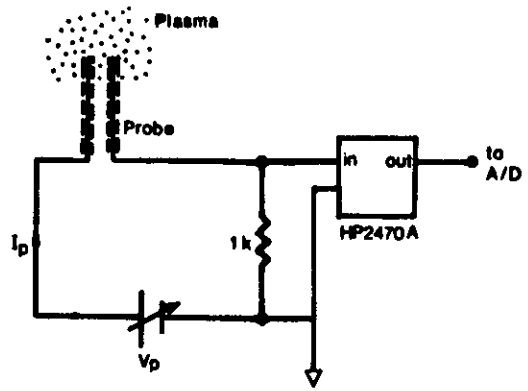

Fig. 2: Experimental set-up of the double Langmuir probe measurement of a plasma.

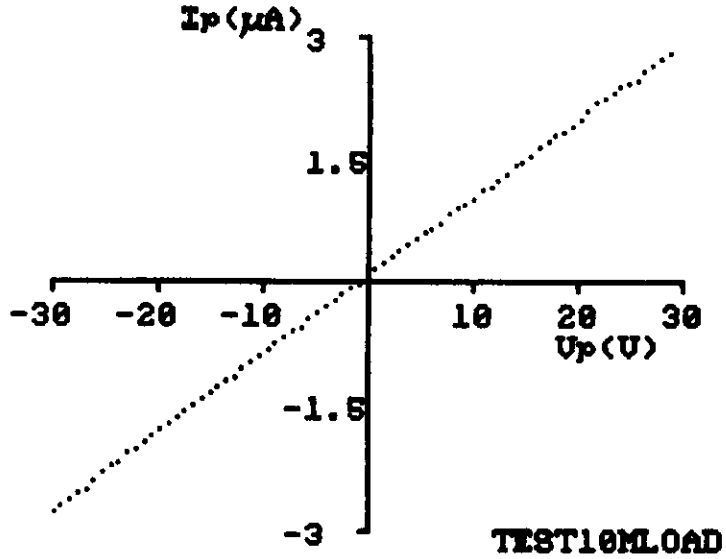

Fig. 3: Ohm's Law simulation test of the microcomputer-controlled Langmuir probe.

Pulsed Langmuir Probe

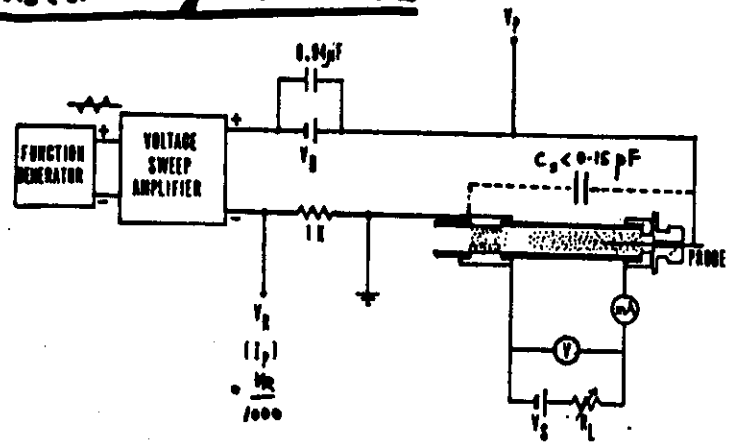

Glow Discharge and Pulsed Langmuir Probe System

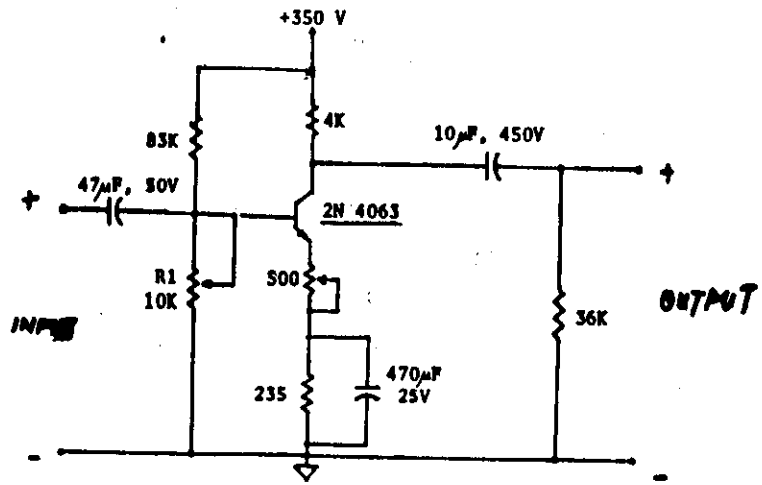

Amplifier to supply voltage sweep to probe
(M.D.Friedman, Rev. Sci. Instrum., 42, 963 (1971))

Acknowledgement

The author is grateful to the Alexander von Humboldt Stiftung of the Federal Republic of Germany for a travel grant to attend this college. He is also grateful to the Institut für Plasmaforschung, Universität Stuttgart for providing the various facilities in the preparation of these lectures.

References

1. 'Laser and Plasma Technology', ed. S.Lee, B.C.Tan, C.S.Wong and A.C.Chew. World Scientific Publishing co., Singapore(1985).
2. 'Plasma Diagnostic Techniques', ed. R.H.Huddlestone and S.L. Leonard. Academic Press, New York(1965).
3. "Rogowski coils: theory and experimental results", V.Nassisi and A.Luches, Rev.Sci.Instrum. 50, 900(1979).
4. "On the high-frequency response of a Rogowski coil", J.Cooper, Plasma Physics 5, 285(1963).
5. "Rogowski coil for measuring fast, high-level pulsed currents", D.G.Pellinen et al, Rev.Sci.Instrum. 51, 1535(1980).
6. "High frequency Rogowski coil response characteristics", W.Stygar and G.Gerdin, IEEE Trans.Plasma Sci. PS-10, 40(1982).
7. "Simple method of pulsed plasma discharge current analysis", C.S.Wong and S.Lee, J.Appl.Phys. 57, 5102(1985).
8. "Effect of stray inductance on capacitive-voltage divider", C.S.Wong, J.Appl.Phys. 59, 673(1986).

9. "Capacitive voltage divider for high-voltage pulse measurement" W.A.Edson and G.N.Oetzel, Rev.Sci.Instrum. 52, 604(1981).
10. "Subnanosecond high-voltage two-stage resistive divider", Z.Y.Lee, Rev.Sci.Instrum. 54,1060(1983).
11. "Simple nanosecond capacitive voltage divider", C.S.Wong, Rev.Sci.instrum. 56, 767(1985).
12. "Simple capacitive probe for high-voltage nanosecond pulses", R.Gratton et al, 57, 2634(1986).
13. "pulsed Langmuir probe technique for measuring the electron energy distribution in glow discharge", O.H.Chin, C.S.Wong and B.C.Tan, paper presented in the Second Tropical College on Applied Physics, Kuala Lumpur(1986). To be published in Proceedings.
14. "Microcomputer-based Langmuir probe system", C.S.Wong, S.H.Saw and O.H.Chin, J.Fiz.Malaysia 6, 115(1985).
15. "Glow discharge measurement using a microcomputer-controlled Langmuir probe", C.S.Wong, paper presented in the Second Tropical College on Applied Physics, Kuala Lumpur(1986). To be published in Proceedings.
16. "Toroidal plasmoids in an electromagnetic shock tube", S.Lee et al, Singapore J.Phys. 3, 75(1986).
17. "Determining nitrogen laser channel parameters", K.H.Kwek et al, J.Fiz.Malaysia 7, 125(1986).

Simple method of pulsed plasma discharge current analysis

C. S. Wong and S. Lee
Plasma Research Laboratory, Physics Department, University of Malaya, Kuala Lumpur 22-11, Malaysia

(Received 13 September 1984; accepted for publication 9 November 1984)

A simple method is proposed to analyze the current waveform of a pulsed plasma discharge from which the voltage waveform and hence the temporal evolution of the plasma inductance can be deduced. As an example, the application of the method to a typical plasma focus discharge is illustrated.

The measurements of the discharge current and the ansient voltage induced across the plasma are essential in ie experimental studies of pulsed plasma discharges. The scharge current can be measured conveniently by using a ogowski coil operated as a current transformer.[1] Such a easurement is considered as the most basic diagnostic in e investigation of a pulsed plasma device. On the other ind, the measurement of the transient voltage across the asma is often found to be more difficult than the current easurement. Recently, several designs of high-perfor-ance capacitive voltage dividers for measuring this tran-nt voltage have been reported.[2,3] In these designs, the vol-ge probes are made an integral part of the plasma device. iis may be difficult to implement in some situations, par-ularly in some existing experiments in small laboratories. order to obtain sufficient information to enable the study the discharge dynamics even without direct measurement the transient voltage, we propose here a simple method to alyze the experimental discharge current waveform from iich the voltage waveform can be deduced. Even in the se where the voltage waveform is being measured experi-ntally, this method of current analysis can be useful as a thod to check the result of the voltage measurement.

Pulsed plasma devices are frequently powered by ca-citor discharge, and a typical equivalent circuit of the dis-rge circuit is as shown in Fig. 1. In this circuit, C is the pacitance of the storage capacitor; L_0 and R_0 are, respec-ly, the inductance and resistance of the circuit external to plasma. The effect of R_0 is usually negligible as com-ed to the effect of L_0. The plasma is represented by a time-ying resistance $R_p(t)$ and a time-varying inductance $L_p(t)$ he circuit.

When the capacitor is charged to a voltage V_0 and then discharged through the circuit, the instantaneous current $I(t)$ that flows through the circuit is described by the circuit equation as follows

$$V_0 - \frac{\int I(t)dt}{C} = \frac{d}{dt}[L(t)I(t)] + I(t)R_p(t), \tag{1}$$

where $L(t) = L_0 + L_p(t)$ is the total inductance of the circuit. Rearranging Eq. (1) gives the voltage across the plasma at any instant as

$$V_p(t) = V_0 - \frac{\int I(t)dt}{C} - L_0\frac{dI}{dt}. \tag{2}$$

This equation can be normalized by introducing the following dimensionless parameters:

$$\tau = t/t_0,\ \iota(\tau) = I(t)/I_0,\ v_p(\tau) = V_p(t)/V_0,$$

where $t_0 = \sqrt{(L_0C)}$ is the capacitor characteristic time and $I_0 = V_0\sqrt{(C/L_0)}$ is the short-circuited peak current. The normalized form of Eq. (2) is

$$v_p(\tau) = 1 - \int \iota d\tau - \frac{d\iota}{d\tau}. \tag{3}$$

Hence the instantaneous transient voltage induced across the plasma of a pulsed plasma discharge can be deduced if the explicit form of its current waveform is known. In practice, the form of $\iota(\tau)$ in Eq. (3) can be obtained by digitizing and then curve-fitting the measured current waveform. This will be illustrated in the following by analyzing the current waveform of a typical plasma focus discharge using the method outlined above.

A typical set of current and voltage waveforms obtained for the University of Malaya Dense Plasma Focus I (UMDPFI)[4] is shown in Fig. 2. The current waveform has been carefully traced onto a graph paper and digitized to produce a set of points (τ, ι) to be curve-fitted into polynomial of $\iota(\tau)$. We shall confine ourselves to the interval between $\tau = 0$, to $\tau = 1.628$, where the current has reached the minimum of the dip.

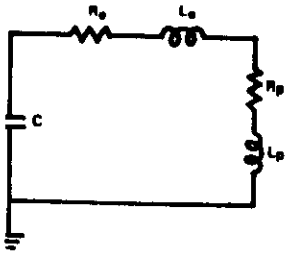

FIG. 1. Equivalent circuit of a pulsed plasma discharge.

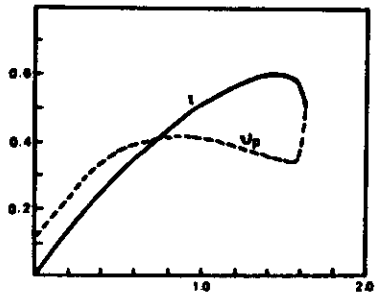

FIG. 2. Experimental current and voltage waveforms (in normalized forms) of a typical plasma focus discharge.

Using the least-square curve-fitting technique, we obtain the following two polynomials of $\iota(\tau)$ for two time regimes:

Regime I. $\tau = 0$–1.54 (positive gradient),

$$\iota(\tau) = -2.8169\times10^{-5} + 0.9303\tau - 1.60595\tau^2 + 2.7603\tau^3 - 1.5817\tau^4 - 0.6485\tau^5 + 0.4259\tau^6 + 0.4689\tau^7 - 0.0966\tau^8 - 0.2278\tau^9 + 0.0832\tau^{10}; \tag{4}$$

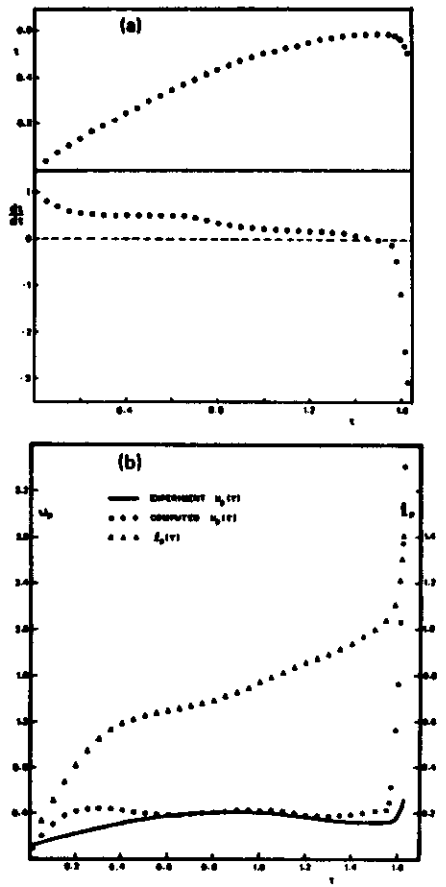

FIG. 3. Results obtained from the analysis of the plasma focus discharge current waveform in Fig. 2. (a) The curve-fitted $\iota(\tau)$ and the corresponding $d\iota/d\tau$. (b) Comparison of the experimental and the computed voltage waveforms and the temporal evolution of the focus tube inductance by assuming an inductive model for the focus discharge.

Regime II. $\tau = 1.54$–1.628 (current-dip, negative gradient)

$$\iota(\tau) = -161.88 + 144.628\tau + 60.389\tau^2 - 24.935\tau^3 - 11.016\tau^4 - 41.092\tau^5 + 15.713\tau^6 + 4.649\tau^7 + 4.363\tau^8 - 2.825\tau^9. \tag{5}$$

It should be noted from these two polynomials that (i) at $\tau \approx 0$, $\iota \simeq 0$ which is expected experimentally; (ii) it can be deduced from Eq. (4) that $d\iota/d\tau = 0.9309$ at $\tau = 0$ which is close to unity; (iii) the value of ι at $\tau = 1.54$ is calculated to be 0.5935 from Eq. (4) and 0.6013 from Eq. (5) which are in good agreement; and (iv) similarly, the value of $d\iota/d\tau$ at $\tau = 1.54$ is calculated to be -4.3×10^{-3} from Eq. (4) and 0.064 from Eq. (5) which can both be approximated to zero. These considerations, together with point by point comparison of the computed and experimental values of ι at various τ indicates that the two polynomials (4) and (5) are accurate representation of the current waveform in the two respective time regimes.

The results obtained from the analysis of the current waveform in Fig. 2 are presented in Fig. 3. The curve-fitted current waveform, together with the corresponding $d\iota/d\tau$ are shown in Fig. 3(a); whereas the voltage waveforms, both computed and experimental, are shown in Fig. 3(b). The computed voltage waveform shows three distinctive regions: (i) the initial slow rise from $\tau = 0$ to $\tau = 0.25$, (ii) the roughly flat plateau region from $\tau = 0.25$ to $\tau = 1.54$, and (iii) the sharp spike which occurs from $\tau = 1.54$ to $\tau = 1.628$. In the measured voltage waveform, however, the voltage is seen to rise more slowly than the computed one, especially in the region of the sharp voltage spike. At the tip of the voltage spike, the measured value is only 0.53 whereas the computed value is as high as 3.4. This is believed to be due to the inadequate response of the probe used.[5] The features of the voltage waveform computed from the current analysis in fact resemble those observed by others,[6,7] although their observed voltage spikes are still low compared to our computation.

With the measured current waveform (curve-fitted into polynomials) and the voltage waveform computed as described above, the temporal evolution of the focus tube inductance can be deduced if an inductive discharge model is assumed. In terms of $v(\tau)$ and $\iota(\tau)$, the normalized form of the tube inductance is given by

$$l_p(\tau) = \frac{\int v_p(\tau)d\tau}{\iota(\tau)}. \tag{6}$$

This has been computed for the example considered here and the result obtained is shown in Fig. 3(b). The sharp rise in l_p corresponding to the current dip is a feature commonly observed for a typical plasma focus discharge. The rise in the focus tube inductance at the start of the discharge is unexpected from a consideration of the focus dynamics. This is probably due to the fact that at the start of the discharge, the tube resistance is not negligible and hence the inductive model is not valid. This tube resistance, however, will soon drop to a negligibly low level as the plasma is heated up. This is most likely to occur during the lift-off phase of the focus discharge dynamics.

We thank T. Y. Tou for providing the set of current and voltage waveforms of the UMDPFI for the above analysis.

 0021-8979/85/115102-03$02.40

[1]S. L. Leonard, in *Plasma Diagnostic Techniques*, edited by R. H. Huddlestone and S. L. Leonard (Academic, New York, 1965), Chap. 2.
[2]C. A. Ekdahl, Rev. Sci. Instrum. 51, 1645 (1980).
[3]W. A. Edson and G. N. Oetzel, Rev. Sci. Instrum. 52, 604 (1981).
[4]Parameters of the UMDPFI are listed in *World Survey of Major Activities in Controlled Fusion Research*; Nucl. Fusion Suppl. (IAEA, Vienna, 1982).
[5]S. Lee, C. S. Wong, A. C. Chew, T. Y. Tou, and Jalil Ali, Singapore J. Phys. 1, 75 (1984).
[6]A. Bernard, A. Coudeville, A. Jolas, J. Launspach, and J. de Mascureau, Phys. Fluids 18, 180 (1975).
[7]G. Decker, W. Kies, and G. Pross, Phys. Fluids 26, 571 (1983).

Effect of stray inductance on capacitive-voltage divider

C. S. Wong
Plasma Research Laboratory, Physics Department, University of Malaya, Kuala Lumpur 22-11, Malaysia

(Received 29 May 1985; accepted for publication 8 July 1985)

The effect of stray circuit inductance on the response of a capacitive-voltage divider to fast-rising voltage pulses is investigated. Results obtained from the analysis of the capacitive divider's equivalent circuit indicate an upper-frequency limit of only 1% of the natural frequency of the circuit.

The capacitive-voltage divider is now being widely used in many laboratories for measuring high-transient voltage pulses such as those encountered in pulsed plasma experiments.[1–3] It is a common practice to design the capacitive-voltage divider as an integral part of the device studied so as to minimize the stray inductance. However, it has been pointed out by Fawkes and Rowe[4] that even a stray inductance of a few hundredths of a microhenry was sufficient to cause nonlinearity in the high-frequency response of this type of voltage divider. Hence the effect of the stray inductance must be taken into account in any realistic design consideration of the capacitive divider. This is particularly important in the measurements of the extremely sharp voltage spikes of possibly less than 10-ns rise times in the plasma focus[5] and in the vacuum spark.[6]

Ideally, the capacitive-voltage divider consists of only two components: capacitors C_1 and C_2. The attenuation factor of the divider is given by

$$V_0/V_i = C_1/(C_1 + C_2), \tag{1}$$

where $C_1 < C_2$. For such an ideal situation, the rise time of the voltage divider is only limited by the transit time of the voltage signal between the output and input terminals. The presence of leakage resistances across the capacitors only affects the low-frequency response of the capacitive divider. Since C_1 and C_2 are usually in the picofarad range, the presence of a stray resistance of milliohm magnitude in series with the capacitors will have practically no effect on the divider's response. This is due to the fact that the RC time constant of such a circuit is only of the order of 10^{-15} s, which is much shorter than the time scale of any possible transient phenomenon that may be studied in the laboratory.

On the other hand, the presence of a stray inductance in the divider's circuit may result in the output voltage waveform being superimposed with high-frequency ringing due to the natural LC oscillation; and the response of the divider thus becomes nonuniform.

The equivalent circuit of an imperfect capacitive-voltage divider consisting of a stray inductance L_s and a stray resistance R_s is represented as shown in Fig. 1. Its circuit equation can be written as

$$L_s \frac{d^2Q}{dt^2} + R_s \frac{dQ}{dt} + \frac{Q}{C} = V_i, \tag{2}$$

where Q is the instantaneous charge flow in the circuit and C is the effective capacitance given by

$$C = C_1C_2/(C_1 + C_2).$$

For simplicity, a sinusoidal input voltage [$V_i = V_m \sin(\omega t)$ where V_m is the peak voltage and ω is the frequency] has been chosen so that a simple analytical solution can be obtained for Eq. (2). For a more general analysis of the circuit, the method of Laplace transform may be used.

Equation (2) can be normalized using the following dimensionless parameters:

$$\tau = t/\sqrt{(L_sC)}; \quad q = Q/Q_0; \quad \delta_s = R_s/\sqrt{(L_s/C)};$$

 0021-8979/86/020673-03$02.40

$\gamma = \omega/\omega_0$; $\omega_0 = 1/\sqrt{LC}$; $Q_0 = CV_m$.

The normalized circuit equation thus obtained is

$$\frac{d^2q}{d\tau^2} + \delta_s \frac{dq}{d\tau} + q = \sin(\gamma\tau). \tag{3}$$

γ is the characteristic parameter of the circuit while δ_s is the damping factor. The solution of Eq. (3) above gives $q(\tau)$, the normalized instantaneous charge that is flowing in the circuit. The output voltage across C_2 can then be computed as

$$v_0(\tau) = \beta q(\tau), \tag{4}$$

where $\beta = C_1/(C_1 + C_2)$ is the ideal attenuation factor of the capacitive divider. It must be pointed out that in this case L_s represents the total inductance of the circuit considered. If part of this inductance is across the output terminals in series with C_2, then the output voltage becomes

$$v_0(\tau) = \beta q(\tau) + k\,(d^2q/d\tau^2), \tag{4a}$$

where k is a number less than unity. The response characteristics of the divider in this configuration is, however, identical to that represented by Fig. 1.

Equation (3) above has three possible solutions depending on the value of δ_s. The three regimes of δ_s are

(a) $\delta_s = 2$ (critically damped);
(b) $\delta_s < 2$ (underdamped); and
(c) $\delta_s > 2$ (overdamped).

In the case of the capacitive-voltage divider considered here, $C \sim pF$; $R_s \sim m\Omega$; and for $L_s \sim nH$, $\delta_s \sim 10^{-5}$ which is much less than 2. Thus the situation here can be approximated to the case of zero damping. Taking $\delta_s = 0$, the solution of Eq. (3) can be written as

$$q(\tau) = A\ [\sin(\gamma\tau) - \gamma\sin(\tau)], \tag{5}$$

where $A = 1/(1-\gamma^2)$. It can be seen from Eq. (5) that for small γ, we have for $0 < \tau < \pi/\gamma$,

$$q(\tau) \simeq \sin(\gamma\tau).$$

This corresponds to the situation of negligible stray inductance ($\omega \ll \omega_0$) where the response of the divider can be considered to be instantaneous.

On the other hand, for large γ, the second term of Eq. (5) becomes important and for sufficiently large γ, it may even dominate over the first term. Under such a condition, the LCR circuit will oscillate at its natural frequency ω_0 after being perturbed by the high-frequency input voltage. The divider, therefore, is unable to follow the temporal development of the input voltage.

From the above discussion, it is clear that the capacitive-voltage divider will be able to give perfect response only if there is no stray inductance present in its circuit. Since there will inevitably be some amount of stray inductance in the circuit of a practical capacitive divider, it is important to determine the upper-frequency limit of a particular divider setup. This can be done by an investigation of the divider's response for various values of γ.

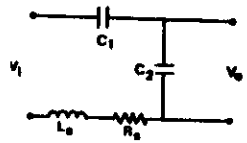

FIG. 1. The equivalent circuit of an imperfect capacitive-voltage divider with stray inductance and stray resistance.

The output waveform of the capacitive divider has been computed from Eqs. (4) and (5) for various values of γ and are shown in Figs. 2(a)–(d). It can be seen from Fig. 2(a) that the output waveform for $\gamma = 0.3$ has been severely distorted. For smaller γ, the output waveform becomes more sinusoidal but it is superimposed with a high-frequency ringing as can be seen from Fig. 2(b). For $\gamma = 0.01$, the output waveform can be considered to be a reasonably accurate reproduction of the input waveform, despite the fact that small-amplitude but high-frequency oscillation is still present [Fig. 2(c)].

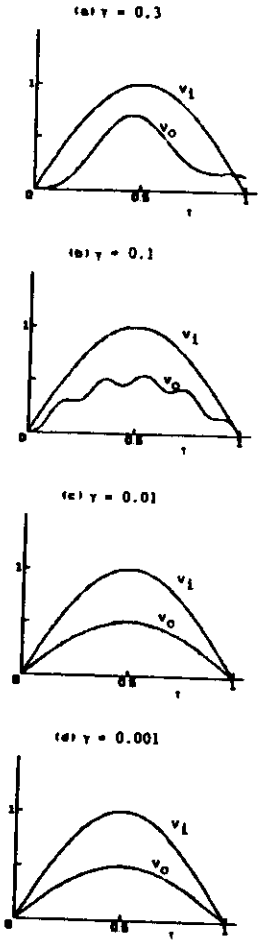

FIG. 2. The input (v_i) and output (v_0) voltage waveforms of an undamped capacitive voltage divider for various values of γ for $\beta = 0.5$. (a) $\gamma = 0.3$; (b) $\gamma = 0.1$; (c) $\gamma = 0.01$; and (d) $\gamma = 0.001$.

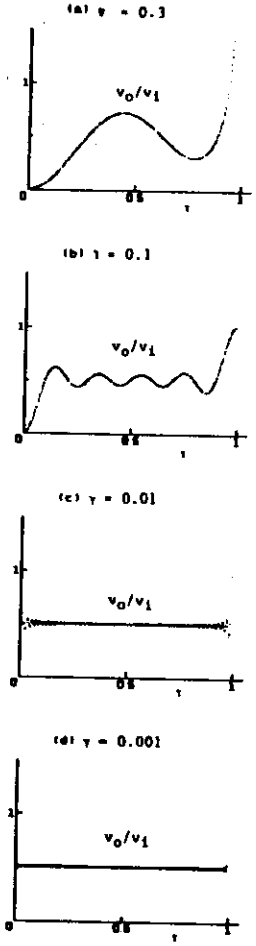

FIG. 3. Plots of v_0/v_i corresponding to the results shown in Fig. 2.

The above description of the response of the imperfect capacitive-voltage divider can be further clarified by looking at the time evolution of the ratio v_0/v_i as shown in Fig. 3(a)–3(d). Ideally, one expects v_0/v_i to be constant and equal to β. This is almost true in the case of $\gamma = 0.001$ [Fig. 3(d)]. In the case of $\gamma = 0.01$, the nonuniform response of the divider gives rise to oscillation of the value of v_0/v_i about the level of 0.5 and this oscillation is most severe near $\tau = 0$ and $\tau = 1$ where $v_0 \to 0$. For the main portion of the plot of v_0/v_i against τ, the value of v_0/v_i oscillates about 0.5 with an amplitude of approximately 0.01.

From the above discussion, it seems reasonable to fix the upper limit of γ at 0.01 for a practical capacitive divider setup. Hence the condition for optimum response of the capacitive divider can be expressed as

$$\omega < 0.01\ \omega_0.$$

For a divider with $C \sim$ pF and $L_s \sim$ nH, we have

$$\omega < 10^8 \text{ rad/s}.$$

Equivalently, the fastest input pulse rise time that the capacitive divider can respond to with sufficient accuracy is

$$t_r > 10 \text{ ns}.$$

The condition for optimum response derived above provides a useful guideline for the design of a capacitive-voltage divider for the measurement of fast voltage pulses. It is clear that in order to relax the constraint on the minimum stray inductance that may be introduced, it is necessary to make C, the overall capacitance, small. In practice, the overall capacitance of the divider is limited to a value governed by the stray capacitance of the setup, which is usually of the order of pF. On the other hand, in order to increase the attenuation factor of the divider, it is required to keep C_2 large compared to C_1. This is usually limited by geometrical constraint. In many applications of the capacitive-voltage divider, water, which has a dielectric constant of $\simeq 80$, is used as dielectric for the capacitor C_2. This may, however, make the capacitor more leaky than those using material such as Mylar as the dielectric, thus affecting the low-frequency limit of the divider.

The author is grateful to Professor S. Lee and Dr. S. P. Chia for their enthusiasm and useful discussions. This work is supported by an F-grant of the University of Malaya (F31/79).

[1] C. A. Ebdahl, Rev. Sci. Instrum. 51, 1645 (1980).
[2] W. A. Edson and G. N. Oetzel, Rev. Sci. Instrum. 52, 604 (1981).
[3] C. S. Wong, Rev. Sci. Instrum. 56, 767 (1985).
[4] W. R. Fawkes and R. M. Rowe, IEEE Trans. Instrum. Meas. IM-15, 284 (1966).
[5] S. Lee, C. S. Wong, A. C. Chew, T. Y. Tou, and Jalil Ali, Singapore J. Phys. 1, 75 (1984).
[6] C. S. Wong, J. Fiz. Malaysia 5, 23 (1984).

Simple nanosecond capacitive voltage divider

C. S. Wong

Plasma Research Laboratory, Physics Department, University of Malaya, Kuala Lumpur 22-11, Malaysia

(Received 2 January 1985; accepted for publication 17 January 1985)

The construction of a simple and inexpensive capacitive voltage probe by using coaxial cable is described. The probe has been tested to a frequency response of better than 30 MHz for sinusoidal voltage input and a rise time of < 20 ns for single-pulse input. The probe is ideal for applications in small experiments involving low-energy and high-voltage capacitor discharge of nanosecond rise time.

The capacitive voltage divider is now being widely used in many laboratories to monitor the transient voltage pulses encountered in various plasma and laser experiments. Several successful designs of the capacitive voltage probe have been reported.[1-4] This note describes an extremely simple version of the capacitive voltage divider which can be made out of coaxial cable. Such a voltage probe can be incorporated into small plasma and laser devices or some fast pulsed electronic circuits to provide an inexpensive method of measuring nanosecond voltage pulses in these devices with sufficient accuracy.

Ideally, a capacitive voltage divider consists of two capacitors connected in series as shown in Fig. 1 (a). In the present design, these capacitors are made from a single coaxial cable as shown in Fig. 1 (b). The capacitor C_1 is formed by embedding a short length (l_1) of the inner conductor of the cable, together with the insulating polythene tube, into the body of the high-voltage component of the discharge system; while the rest of the length of the coaxial cable (l_2) acts as the capacitor C_2. The attenuation ratio (output:input) of this divider is

$$\beta = C_1/(C_1 + C_2).$$

In this case, C_2 is connected directly across the input of the oscilloscope which has a typical input resistance of 1 MΩ. If required, the attenuation can be increased tenfold by connecting a 10 MΩ resistor in series to the oscilloscope's input.

The response characteristics of the above capacitive voltage divider is determined primarily by C_2. At the low-frequency end, the response of the probe is limited by the decay time constant of $C_2 R_i C_2$, where R_i is the input resistance of the oscilloscope used; while the high-frequency end is limited by the transit time for signal to travel along the length of C_2. For a single-voltage pulse of rise time t_r, the probe will be able to respond accurately if

$$t_r > (l_2/v),$$

where v is the velocity of propagation of electrical signal along the coaxial cable, which is approximately 2×10^8 m/s.

The probe constructed for illustration here uses a RS Uniradio 43 coaxial cable. This cable is rated at 21 kV dc, 2.6 kV peak rf(cw), and has a capacitance of 100 pF/m in its manufactured form. With l_2 fixed at 1 m, $C_2 = 100$ pF, and the ultimate limit of the probe's response time is

$$t_r > 5 \text{ ns}.$$

The attenuation ratio of the probe can be calculated if C_1 is known. In practice, this ratio is obtained by calibrating the probe with a voltage of known amplitude.

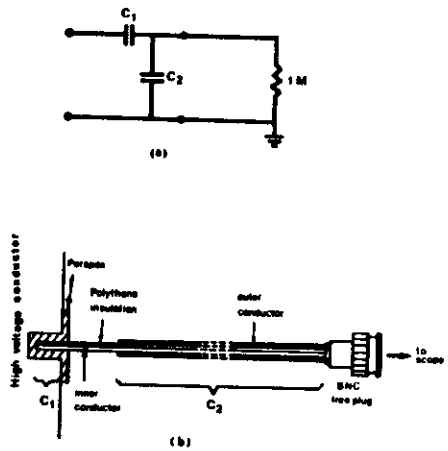

FIG. 1. (a) The equivalent circuit of the capacitive voltage divider connected directly to the oscilloscope, (b) schematics of the capacitive voltage divider which is made from a single coaxial cable.

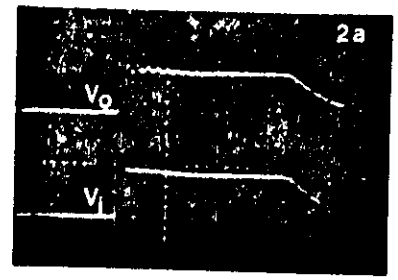

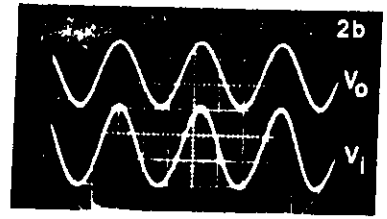

FIG. 2. (a) The response of the capacitive voltage divider to a 20-ns rise-time step voltage function. Upper trace is the output waveform V_o while the lower trace is the input waveform V_i. (Vertical scale: 0.2 V/cm for V_o; 20 V/cm for V_i. Horizontal scale: 100 ns/cm. (b) the response of the capacitive voltage divider to a 30-MHz sinusoidal waveform. Upper trace is the output waveform while lower trace is the input waveform. (Vertical scale: 0.5 V/cm for V_o; 50 V/cm for V_i. Horizontal scale: 10 ns/cm.)

Figure 2 (a) shows the response of the present capacitive voltage probe to a square pulse of 20-ns rise time. It can be seen that the probe is able to respond accurately to the voltage pulse. The ringing at the plateau region of the voltage pulse is probably due to the presence of a stray inductance which is contributed by the cable itself. Similarly, Fig. 2 (b) shows the accurate response of the probe to a 30-MHz sinusoidal waveform with peak-to-peak amplitude of 130 V. The attenuation ratio of the probe calculated from these measurements is 1/110.

The pulse hold-off voltage of the probe is determined mainly by the insulation of C_1. In this design, the insulation of C_1 is enhanced by adding a small Perspex cap to cover the part of the coaxial cable which is embedded in the high-voltage conductor as shown in Fig. 1 (b). In this manner the probe's hold-off voltage can be considerably higher than the rated values. However, since it is desirable to keep the length of C_2 short in order to minimize the stray inductance as well as the signal transit time, the measuring oscilloscope must be stationed close to the high-voltage point of the device being studied. It is therefore recommended that the probe be used for experiments involving low-energy capacitor discharge (<20 kV). Despite this limitation, the probe can be considered a useful tool for a number of plasma and laser experiments as well as some pulsed control electronic circuits

 0034-6748/85/050767-03$01.30

where nanosecond voltage pulses of kilovolts amplitudes need to be measured. The simplicity of the probe's construction ensures its quick implementation with minimum expenses.

[1]G. E. Leavitt, J. D. Shipman, Jr., and I. M. Vitkovitsky, Rev. Sci. Instrum. 36, 1371 (1965).
[2]N. W. Harris, Rev. Sci. Instrum. 48, 961 (1974).
[3]C. A. Ekdahl, Rev. Sci. Instrum. 51, 1645 (1980).
[4]W. A. Edson and G. N. Oetzel, Rev. Sci. Instrum. 52, 604 (1981).

0034-6748/85/050700-03$01.30

J. Fiz. Mal. 6, 115 (1985)
Research Note

MICROCOMPUTER-BASED LANGMUIR PROBE SYSTEM

C.S. WONG, S.H. SAW AND O.H. CHIN
Plasma Research Laboratory
Physics Department
University of Malaya
Kuala Lumpur 22-11
Malaysia

Abstract

A simple microcomputer-based data acquisition system is set up to obtain the I-V characteristic of the Langmuir probe. The system is ideal for extensive probe data collection in the study of steady-state plasmas.

The Langmuir probe is a simple but effective tool for the diagnostic of fairly large volume, relatively cold and low density plasmas. From the I-V characteristic of the probe, plasma parameters such as the electron temperature, electron density, space potential and electron energy distribution can be deduced. For a time-varying plasma, the pulsed Langmuir probe[1-4] must be used. In the case of a steady-state plasma, it is usually sufficient to use the point-by-point technique, although the pulsed method can also be employed. However, the process of obtaining the Langmuir probe characteristic by the point-by-point method and its analysis is tedious and time-consuming if it is done manually. This is particularly true in cases where the Langmuir probe is employed as a basic diagnostic and extensive data are required to be collected concurrently with other diagnostics of the plasma.

In this note, a simple microcomputer-based data acquisition system for the Langmuir probe is described. The system employs an Apple-II microcomputer to control the variation of the probe's bias potential as well as to monitor the probe current automatically.

The data acquisition system consists of a 64k RAM Apple-II microcomputer which is supported by a high-resolution CRT display unit; two mini floppy disk-drives and a dot matrix printer with high-resolution graphic capability (Fig. 1). Data acquisition is done via a multi-channel A/D + D/A interface card (Mountain Computer Inc.) which can be plugged directly into the expansion slot of the Apple-II. This interface card provides 16 cannels each of analog-to-digital and digital-to-analog converters. The range of its analog input/output level is −5V to +5V, with a digital equivalence of 0 to 255.

The experimental set-up of the microcomputer-based double Langmuir probe measurement of a plasma is as shown in Fig. 2. A 1 kΩ resistor is connected in place of the usual microammeter for measuring the probe current, Ip. The potential drop across the 1 kΩ resister is expected to be of the order of mV only and hence it must be amplified before it is fed into an A/D channel of the computer. This is done by using a HP2470A data amplifier.

The probe potential Vp is supplied by using the HP467A power amplifier acting as a variable power supply. The output of the power amplifier can be varied within the range of −30V to +30V by applying a voltage of −3V to +3V to its input. Thus when used in conjunction with a digital-to-analog converter, the HP467A power amplifier functions as a low voltage digitally controlled power supply. This arrangement is good enough for the present purpose. If higher voltages are required, the digitally controlled power supply described by Fanelli and Merangelli[5] may be employed.

It is the present intention to apply the above microcomputer-controlled Langmuir probe system to study the plasma of a dc glow discharge. However, in order to test the reliability of the system, a simulation experiment is first performed by replacing the plasma with a 10 MΩ resistor

(±10%). For such a simulation system, the current flow in the circuit varies linearly with voltage (Ohm's Law) This has been obtained as shown in Fig. 3. The slope of the straight line obtained is 10.5 MΩ which is consistent with the resistance of the load used.

As an example to illustrate the operation of the microcomputer-controlled Langmuir probe system, the double probe characteristic of a hot-cathode dc glow discharge is obtained as shown in Fig. 4. The feature of this probe characteristic is typical to that obtained with a contaminated and non-symmetrical double probe. It is well known[6] that surface contamination of the Langmuir probe has the effect of smoothing out the "knee" of the characteristic; whereas the intercept of the curve on the V_p-axis at point C is caused by the difference in the plasma potentials at the locations of the two probes. The electron temperature of the plasma can be determined from the slope of the characteristic at point C where I_p=0. This has been obtained to be T_e=(2.0 ± 0.2) eV in the above case, which is typical for the glow discharge plasma considered here.

We have illustrated above the operation of a microcomputer-based Langmuir probe system for the measurement of the electron temperature of a glow discharge plasma. As can be seen from Fig. 4, more points at small voltage increments of 0.4V have been obtained for a single characteristic, which is not possible if the same procedures are performed manually. Thus the utilization of microcomputer in Langmuir probe measurement has greatly enhanced its accuracy and effectiveness as a basic diagnostic in the study of steady-state plasmas.

Acknowledgement

We are grateful to Professor Lee Sing for encouragement and support. This work is supported by a F-grant of the University of Malaya (F 31/79).

References

1. W.D. Friedman, Rev. Sci. Instrum. 42, 963 (1971).
2. J. Lacoste and K. Dimoff, Rev. Sci. Instrum. 44, 1278 (1973).
3. B.A. Hoegger and A. Bullard, Rev. Sci. Instrum. 51, 735 (1980).
4. C.S. Wong, J. Fiz. Mal. 5, 121 (1984).
5. A.M. Fanelli and B. Marangelli, J. Phys. E: Sci. Instrum. 16, 727 (1983).
6. J.D. Swift and M.J.R. Schwar, *Electric Probe for Plasma Diagnostic*, Iliffe Books, London (1971).

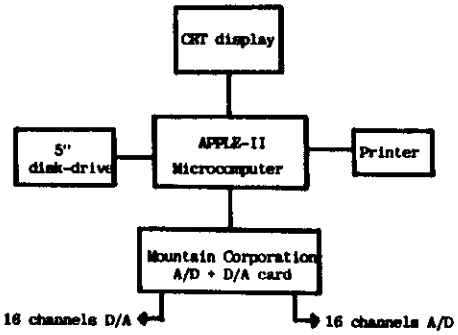

Fig. 1: Schematic of the microcomputer-based data acquisition system.

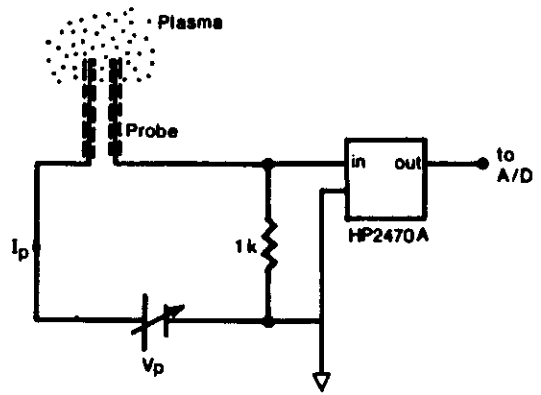

Fig. 2: Experimental set-up of the double Langmuir probe measurement of a plasma.

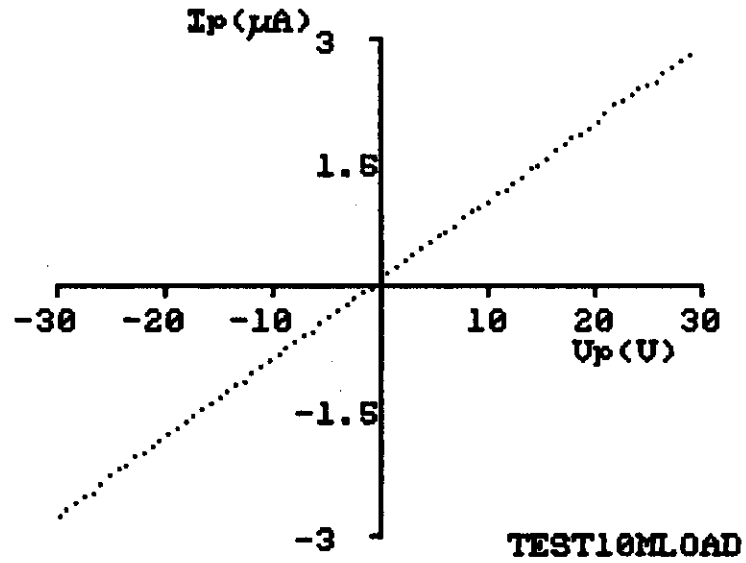

Fig. 3: Ohm's Law simulation test of the microcomputer-controlled Langmuir probe.

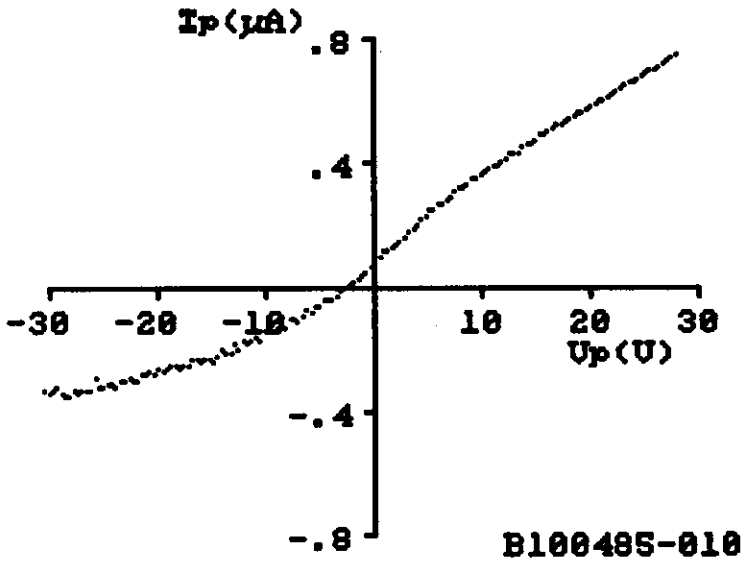

Fig. 4: A double probe characteristic of the hot-cathode dc glow discharge plasma obtained by the computer.

SECOND TROPICAL COLLEGE ON APPLIED PHYSICS

EXPERIMENT

GLOW DISCHARGE MEASUREMENT USING A MICROCOMPUTER-CONTROLLED LANGMUIR PROBE

C.S.Wong

1. Aim of the experiment.

In the glow discharge experiment[1] of the First Tropical College on Applied Physics, the measurement of the Langmuir probe characteristic had been obtained by the point-by-point manual method. In the present experiment, this will be obtained by a microcomputer-controlled data acquisition system.

2. The glow discharge system.

The glow discharge tube used in this experiment is of the cold cathode type consisting of ring electrodes as shown in Fig. 1. The tube is pumped to a base pressure of ~ 10^{-4} mbar before helium gas is filled in. With this discharge tube, steady discharge can be maintained at an interelectrode voltage drop of 400 to 800 volts in helium at filling pressure in the range of 2 to 20 mbar. In this experiment, the discharge is maintained at 10 mbar helium. For a discharge current of I_a = 50 mA, the voltage drop across the electrodes is 675 V.

The glow discharge circuitary used in this experiment is shown in Fig. 2. The discharge current can be controlled by

adjusting either the limiting resistor R_L or the power supply output V_s. The voltage drop across the electrodes and the discharge current are monitored by analog voltmeter and ammeter.

3. The Langmuir probe.

The Langmuir probe is made from molybdenum wire of 1 mm diameter. The Mo wire is inserted into a small thin-wall glass tube of inner bore diameter slightly more than the wire until the tip of the wire become flush with one end of the glass tube. The Mo wire together with the glass tube is then heated in gas flame until the Mo wire becomes red-hot and the glass tube becomes soften and begins to shrink. This procedure will ensure that there is no space left between the Mo wire and the inner wall of the glass tube. The tip of the wire-glass assembly now forms a plane probe geometry. This probe is supported by inserting it into another glass tube of bigger bore diameter and is introduced into the plasma through a perspex holder from the entrance on the anode(Fig. 1).

4. The microcomputer-controlled data acquisition system.

The data acquisition system consists of a 64k RAM Apple-II microcomputer which is supported by a high-resolution CRT display unit, two mini floppy disk-drives and a dot matrix printer with high-resolution graphic capability(Fig. 3). Data acquisition is done via a multi-channel A/D + D/A interface card(Mountain Computer Inc.) which can be plugged directly into the expansion slot of the Apple-II. This interface card provides 16 channels each of analog-to-digital and digital-to-analog converters. The

range of its analog input/output levels is -5V to +5V, with a digital equivalence of 0 to 255. This gives a resolution of not better than 39 mV for the system.

The experimental set-up of the microcomputer-based Langmuir probe measurement of a plasma is as shown in Fig. 2. A 1 kΩ resistor is connected in place of the usual micro-ammeter for measuring the probe current, I_p. The potential drop across the 1 kΩ resistor is expected to be of the order of mV only, and hence it must be amplified before it is fed into an A/D channel of the computer. This is done by using a HP2470A data amplifier.

The probe potential V_p is supplied by using a battery pack connected in series with a HP467A power amplifier acting as a variable power supply. The output of the battery pack can be sellected between 0 to 900 V in step of 22.5 V. The output of the power amplifier can be varied within the range of -30 V to +30 V by applying a voltage of -3 V to +3 V to its input. Thus when used in conjunction with a digital-to-analog converter, the HP467A power amplifier functions as a low voltage digitally controlled power supply. This arrangement is good enough for the present purpose.

5. Experimental procedures.

5.1. Getting the glow.

Before the start of the experiment, the glow discharge tube should have been pumped to a pressure of ~ 10^{-4} mbar. The pump is then cut-off and helium gas is let in to a pressure of 25 mbar(end of scale of the pressure gauge). With only the rotary pump, the gas is evacuated for about 5 minutes to a pressure of ~

10^{-2} mbar. Helium gas is filled in again and the procedure may be repeated two to three times so that a reasonably pure volume of helium is obtained. The pressure of the chamber is finally maintained at 10 mbar of helium.

The power supply V_s is now turn on and its output is increased slowly. Initially, before the gas breaks down, the voltmeter V_a indicates the output voltage of power supply V_s. However, at $V_s \sim 1.2$ kV, gas breakdown will occur and current starts to flow through the discharge tube as indicated by the reading on the milliammeter. V_a now shows the voltage drop across the electrodes and it is less than V_s. A glow should now be visible. Note the shape and the colour of the glow! and also identify the positive column. Is the probe immersed in the positive column of the discharge ? Now adjust R_L or V_s so as to obtain the appropriate current and note down the values of the following quantities :

V_s = volts;

V_a = volts;

I_a = mA; and

P = mbar.

5.2. Determining the suitable starting voltage for the data acquisition.

Depending on its location along the axis of the discharge tube, the floating potential of the probe(ϕ_f) may vary between the range of (V_a-300) to V_a; while the electron retardation region of the probe characteristic lies between ϕ_f and the space potential ϕ_s at the location of the probe. At a probe potential

of $V_p > \phi_s$, electrons will be attracted towards the probe surface, bombarding it to produce a faint glow at the tip of the probe. This glow is used as an indicator to choose the suitable starting probe potential V_B. It is learnt from experience that the suitable starting potential can be fixed at 2 step below the potential above which a glow begins to be visible at the tip of the probe.

5.3. Sweeping the probe potential - determination of the probe characteristic.

We are now ready to obtain a set of the probe characteristic for the helium discharge. The sweeping of the probe potential and the measurement of the corresponding probe current are controlled by using a BASIC programme[FILENAME : DATA ACQUISITION(S)!]. The sequence of operations of this programme is as follows :

(i) At the start of a RUN, the programme will request the user to input various parameters such as V_a, I_a, V_B, P etc and a user created data serial number.

(ii) The programme then proceeds to perform the data acquisition. At each step, the programme sends an analog output, via a D/A channel, to the input terminal of the HP467A power amplifier which then produces an amplified output voltage V_o in series to V_B. Thus the effective probe potential is $V_p = V_o + V_B$. If the amplification factor sellected is x10, then the minimum voltage step-size is 0.39 V. The choice of the most suitable sweep voltage range and the step-size will be obtained after some trial-and-error processes so as the best result is

achieved.

(iii) After the completion of the data acquisition, the programme will request for the input of I_a, V_a and P again. This allows the user to check if these parameters have changed during the data acquisition.

(iv) Upon receiving the requested parameters, the computer begins to print out a listing of the probe data collected (I_p - V_p).

(v) Finally, the programme ask the user to decide if the present set of data collected should be stored into disk memory for further analysis. This allows the user to discard data which are not correct. If a positive reply is given, the programme will store the data under the filename of the data serial number input at the start of the RUN. The programme then resets to the start and it is now ready for the next sequence of data acquisition.

The above sequence of events is illustrated in the flow chart in Fig. 4.

5.4. Plotting the probe characteristic.

Using the data listing obtained in step (iv) of the operation of the data acquisition programme above, the probe characteristic obtained for the helium glow discharge can now be plotted. You may also use the programme PLOT I-V(S) to plot the characteristic. An example of the I-V characteristic plotted by this programme will be shown in Appendix B.

6. Analysis.

From the probe characteristic obtained above, deduce the electron temperature T_e, the electron density n_e and the space potential ϕ_s of the helium positive column. (Refer to Ref.1 for the interpretation of the probe characteristic).

Reference.

1. C.S.Wong, Experiment V: The Glow Discharge Experiment, in "Laser and Plasma Technology" ed. S.Lee, B.C.Tan, C.S.Wong and A.C.Chew. World Scientific Publishing Co., Singapore(1985).

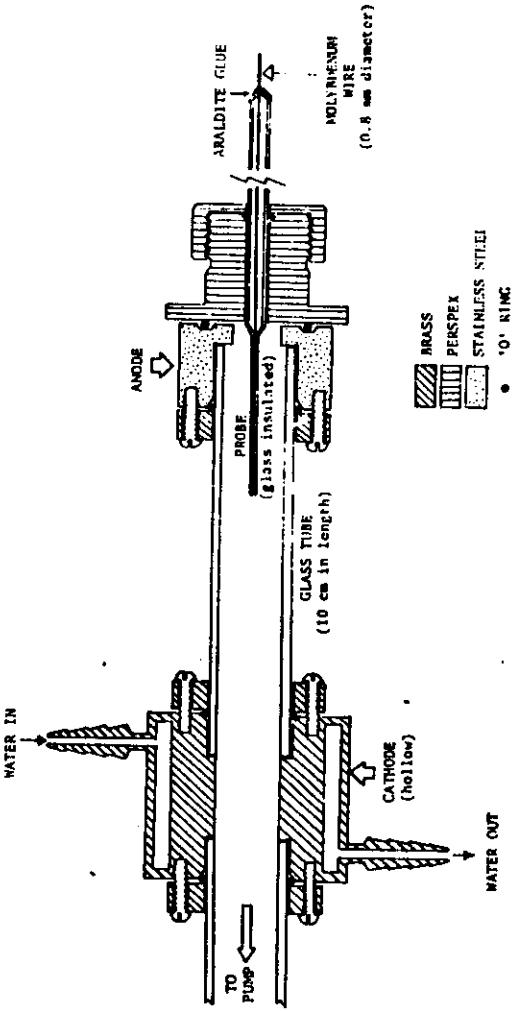

Fig. 1. Schematic of the glow discharge tube.

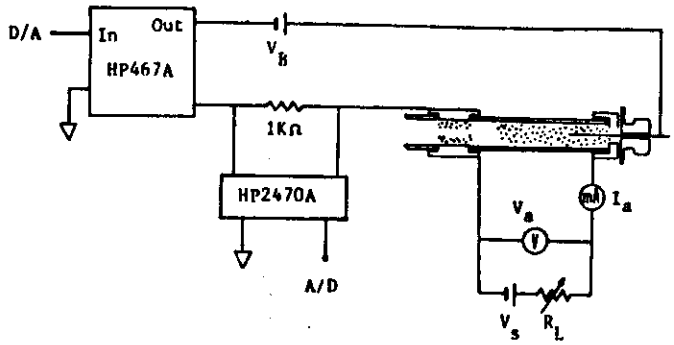

Fig. 2. Experimental set-up of the microcomputer-based Langmuir probe measurement of the glow discharge.

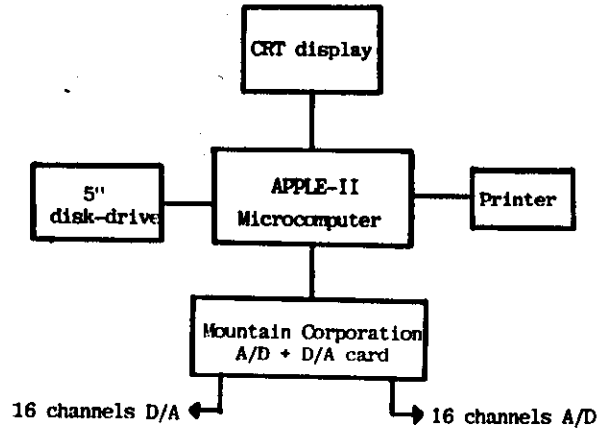

Fig. 3. Block diagram of the data acquisition system.

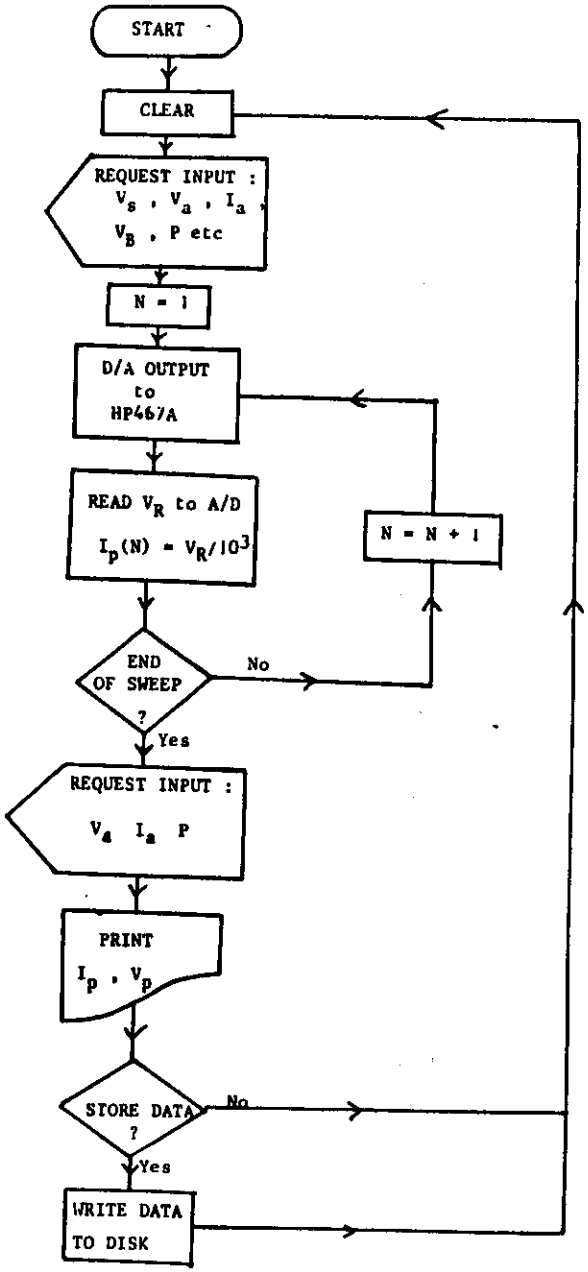

Fig. 4. Flow chart showing the sequence of data acquisition.

Appendix A : Programme listing of DATA ACQUISITION(S).

```
1  TEXT : HOME
10  REM
20  REM       *** NAME: DATA ACQUISITION(S)
30  REM
35  REM  *** DATA ACQUISITION OF THE SINGLE LANGMUIR PROBE
36  REM   *** GLOW DISCHARGE
38  REM
40  REM  ***FOR Vp, USE D/A OUTPUT AMPLIFIED BY HP467A POWER AMP
45  REM
50 M1 = 500: REM  Ip IS AVERAGED OVER M1 DATA
60  DIM IP(256),VF(256)
70  REM
80  REM   A/D+D/A CARD IN SLOT 5
90  REM
100 A = 49370: REM   D/A CH 10 TO OUTPUT Vp
140 S3 = 49360: REM    CHANNEL NUMBER FOR Ip IS 0
260  REM
374  PRINT "****************************************"
376  PRINT "* SINGLE LANGMUIR PROBE MEASUREMENT OF *"
377  PRINT "*            GLOW DISCHARGE            *"
378  PRINT "****************************************"
380  PRINT : PRINT
390  INPUT "DATA SERIAL NUMBER(Bddmmyy-nnn) : ";F$: PRINT
392  INPUT "DISCHARGE VOLTAGE(V) = ";VZ: PRINT
410  INPUT "TYPE OF GAS USED IS ";N$: PRINT
415  INPUT "AMPLIFICATION FACTOR OF POWER AMP = ";PF: PRINT
425  INPUT "RESISTANCE FOR MONITORING Ip(ohms) = ";RI: PRINT
426  INPUT "BASE PROBE POTENTIAL(V) = ";VB: PRINT
427  INPUT "AMPLIFICATION FACTOR OF OP-AMP = ";AF: PRINT
430  INPUT "INITIAL VESSEL PRESSURE(mbar) = ";PI: PRINT
435  INPUT "DISCHARGE CURRENT(mA) = ";MI: PRINT
440  INPUT "MEASURED ANODE POTENTIAL(IN V) = ";MV: PRINT
450  REM
770  PRINT : PRINT "Data acquisition in progress....."
803  PRINT : PRINT
805  REM
806  REM  *** DATA ACQUISITION ***
807  REM
808 II = 0
810  FOR I = 50 TO 140 STEP 2
811 II = II + 1
812  POKE A,I
815  FOR PAUSE = 1 TO 1000: NEXT PAUSE
820 SY = 0
960  FOR J3 = 1 TO M1
970 Y =  PEEK (S3):Y =  PEEK (S3)
980 SY = Y + SY
990  NEXT J3
1260  REM
1270  REM  *** CALCULATIONS
1280  REM
1310 V3 = ((SY / M1) * 10 / 255 - 5)
1320 VP(II) = (I * 10 / 255 - 5) * PF + VB
1330 IP(II) = V3 / (AF * RI)
1425  NEXT I
```

```
1485  HOME
1490  FLASH : PRINT "DATA ACQUISITION COMPLETED": NORMAL
1495  PRINT : PRINT
1500  INPUT "FINAL VESSEL PRESSURE(mbar) = "|PF: PRINT
1502  INPUT "FINAL DISCHARGE CURRENT(mA) = "|FI: PRINT
1504  INPUT "FINAL ANODE POTENTIAL(V) = "|FV: PRINT
1510 P = (PI + PF) / 2
1512 MI = (MI + FI) / 2
1514 MV = (MV + FV) / 2
1520  REM
1530  REM  *** PRINT DATA
1540  REM
1550  PR# 1
1564  PRINT "*************************************************"
1565  PRINT "*                                               *"
1570  PRINT "* SINGLE LANGMUIR PROBE MEASUREMENT OF UMGD-B *"
1575  PRINT "*                SER.NO.: "|F$|"                *"
1580  PRINT "*                                               *"
1590  PRINT "*************************************************"
1592  PRINT : PRINT
1595  PRINT "     Discharge voltage = "|VD|" V"
1596  PRINT "     Discharge current = "|MI|" mA"
1597  PRINT "     Anode potential = "|MV|" V"
1601  PRINT "     Type of gas used is "|N$
1602  PRINT "     Pressure = "|P|" mbar"
1605  PRINT : PRINT
1610  PRINT "Vp(V)"| TAB( 20)|"Ip(uA)"
1620  PRINT "======"| TAB( 20)|"======="
1630  FOR I = 1 TO II
1640  PRINT VP(I)| TAB( 20)|IP(I) * 1E6
1650  NEXT I
1660  PRINT : PRINT
1670  PR# 0
1900  PRINT
1820  INPUT "DO YOU WISH TO STORE THE DATA?(Y/N) "|C$
1825  PRINT
1830  IF C$ = "Y" THEN  GOTO 1850
1840  GOTO 2010
1850  REM
1860  REM  *** TO STORE DATA
1870  REM
1890 D$ =  CHR$ (4): REM  CHR$(4)=CTRL-D
1900  PRINT D$|"OPEN "|F$
1910  PRINT D$|"WRITE "|F$
1920  PRINT II
1930  PRINT P
1940  PRINT MV
1950  PRINT MI
1960  PRINT N$
1970  FOR I = 1 TO II
1980  PRINT IP(I): PRINT VP(I)
1990  NEXT I
2000  PRINT D$|"CLOSE"
2010  RUN
```


Appendix B : An example of the I-V characteristic of the Langmuir probe plotted by the computer.